

Gupta, J., Lin, C.-H., and Chen, Q. 2009. "Flow dynamics and characterization of a cough," *Indoor Air*, 19, 517-525.

Flow Dynamics and Characterization of a Cough

Jitendra K. Gupta^a, Chao-Hsin Lin^b, Ph.D., Qingyan Chen^a, Ph.D.

^aNational Air Transportation Center of Excellence for Research in the Intermodal Transport Environment (RITE), School of Mechanical Engineering, Purdue University, West Lafayette, IN 47907-2088, USA

^bEnvironmental Control Systems, Boeing Commercial Airplanes, Seattle, WA 98124, USA

Abstract

Airborne disease transmission has always been a topic of wide interests in various fields for decades. Cough is found to be one of the prime sources of airborne diseases as it has a high velocity and a large quantity of droplets. To understand and characterize the flow dynamics of a cough can help the control of airborne disease transmission. This study has measured flow dynamics of coughs with human subjects. The flow rate variation of a cough with time can be represented as a combination of gamma-probability-distribution functions. The variables needed to define the gamma-probability-distribution functions can be represented by some medical parameters. A robust multiple linear regression analysis indicated that these medical parameters can be obtained from the physiological details of a person. However, the jet direction and mouth opening area during a cough seemed not related to the physiological parameters of the human subjects. Combining the flow characteristics reported in this study with appropriate virus and droplet distribution information, the infectious source strength by coughing can be evaluated.

Keywords: Airborne infection, airflow, mouth opening, visualization, modeling

Practical Implications:

There is a clear need for the scientific community to accurately predict and control the transmission of airborne diseases. Transportation of airborne viruses is often predicted using Computational Fluid Dynamics (CFD) simulations. CFD simulations are inexpensive but need accurate source boundary conditions for the precise prediction of disease transmission. Cough is found to be the prime source for generating infectious viruses. The present study was designed to develop an accurate source model to define thermo-fluid boundary conditions for a cough. The model can aid in accurately predicting the disease transmission in various indoor environments, such as aircraft cabins, office spaces and hospitals.

1. INTRODUCTION

Transmission of infectious respiratory diseases has always been a topic of wide interests and has received attention from various disciplines for decades (Morawska, 2006). The transmission can happen through direct and indirect contacts or could be airborne. The transmission takes place through the droplets carrying the infectious viruses. Commonly encountered airborne transmitted diseases are cold and influenza and severe one like Severely Acute Respiratory Syndrome (SARS) and avian flu. The Spanish flu of 1918-19 (H1N1) was by far the most lethal flu pandemic of the 20th century. According to the World Health Organization (WHO) estimates, it infected about one-quarter of the global population and took the lives of more than 40 million people (WHO, 2002). A pandemic of avian flu among humans could cost the global economy \$800 billion a year (World Bank, 2005). Not only avian flu could be deadly; there were 8098 people infected by SARS and 774 of them died according to statistics from the (WHO, 2002). The epidemic caused significant social and economic disruption in areas with sustained local transmission of SARS. As people spend most of their time at indoor workplaces, they would very likely be infected by flu or other airborne infectious viruses if there is a pandemic. This indicates a clear need for the scientific community from various disciplines to accurately predict and control the transmission of airborne diseases.

Airborne transmission starts from infectious viruses exhaled from an infected person (Cole et al., 1998). Then the viruses are transported in the air and finally inhaled by a susceptible person. Some have investigated the virus transportation (Holmes et al., 2006) in air but there is no comprehensive literature on exhalation and inhalation characterization. Transportation of airborne viruses is predicted using Computational Fluid Dynamics (CFD) simulations (Holmes et al., 2006) or using benign bacterial virus and biological air sampling technique (Sze To et al., 2008). But CFD simulations are often used as they are inexpensive in comparison with the experiments. They need flow-thermal boundary conditions from the source of infectious viruses. The boundary conditions for exhalation are as follows

- Flow rate and direction
- Mouth or nose opening area
- Temperature
- Size distribution of the virus droplets and quantity of virus in the droplets

These parameters are transient and can have considerable variation among people. The CFD simulations (Zhu et al., 2006, 2006; Zhao et al., 2005) for dispersion predictions have treated these boundary conditions as constant flow rate with assumed direction, temperature, an approximate estimate for the area of the mouth or nose opening. Accurate boundary conditions are important for precise prediction of disease virus transmission.

Exhalation modes include coughing, sneezing, talking, or breathing. Coughing and sneezing processes are the major sources of contaminants as they have higher droplet concentration (Duguid, 1945) compared with the others. But as coughing is a common symptom for most respiratory infections, the present study is focused on developing a model to prescribe the boundary conditions for the coughing process. There is substantial literature on cough droplet size distribution (Duguid, 1945; Fairchild et al., 1987; Papineni et al., 1997; Fenelly et al., 2004; Yang et al., 2007; Hersen et al., 2008; Chao et al., 2009; Morawska et al., 2009) and exhaled air temperature (Hoppe, 1981). Hence this study limited the scope to the flow dynamics of a cough, i.e. flow rate, flow direction, and the area of mouth opening during a coughing process.

2. STATE OF THE ART

2.1 Exhale airflow rate and direction from a cough

Figure 1 shows the typical flow generated from a cough over time. Information about cough flow rate is available from the literature (Leiner et al., 1966; Mahajan et al., 1994; Singh et al., 1995), such as Cough Peak Flow Rate (CPFR), Cough Expired Volume (CEV) that is the area under the curve, and Peak Velocity Time (PVT). The information is of great medical interests (Lamb et al., 1993), but it is not useful as boundary conditions in CFD simulations.

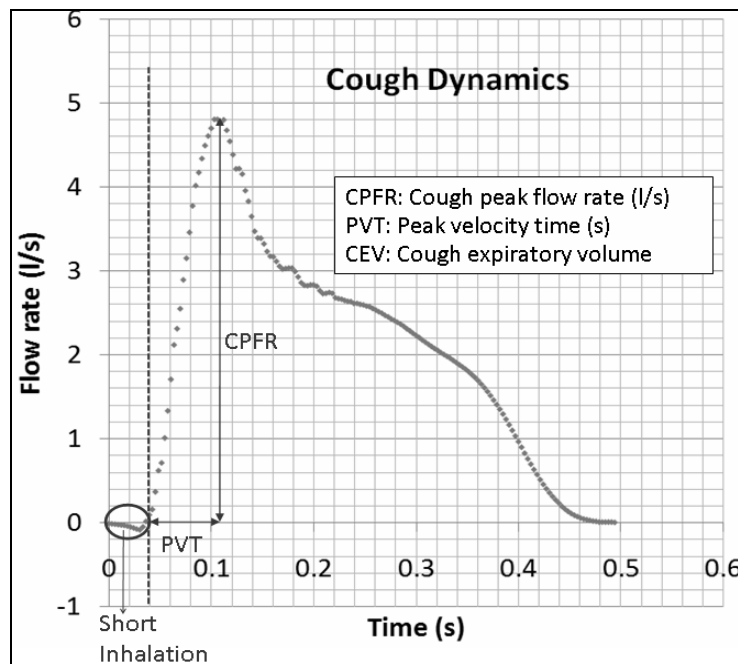


Fig. 1 Cough flow rate variation with time

However, the information provides good insight of the flow behavior of a coughing process. Leiner et al. (1966) correlated CPFR with the height and age of human subjects through a regression analysis. Mahajan et al. (1995) further developed relations between CPFR, CEV and PVT. Later Singh et al. (1995) corrected the relationship between CPFR and PVT for different genders and found the difference caused by the larynx size in male and female. The total cough volume measured by Zhu et al. (2006) had a variation of 0.8-2.2 liter with an average of 1.4 liter which actually was the low end as compared with that from Mahajan et al. (1994), who observed a variation of up to 5 L with an average of about 3 L. Though these studies gave some information on cough but did not quantify the dynamics of the cough profile.

On the other hand, there were a number of studies visualizing the coughing process that could be used to create boundary conditions for CFD simulations. Jennison et al. (1942) visualized cough through high speed photography using strobe (Edgerton et al., 1959). Their main emphasis was on droplet size distribution but he also revealed qualitatively the droplet dispersion to 2-3 feet from mouth. Settles et al. (1995) captured the thermal plume coming out of a cough through Schlieren imaging. But none of these studies could characterize the transient process or direction of the jet. Particle Image Velocimetry (PIV) (Afshari et al., 2002; Badeau et al., 2002, VanSciver; Zhu et al., 2006, 2006; Chao et al., 2009) measurements were also performed to capture the flow field. Mahajan et al. (1995) pointed out that the PVT was in the order of a few milliseconds. Hence to capture the cough jet variation and its direction it becomes essential to have a high frequency of measurements. PIV measurements by Afshari et al. (2002) and Badeau et al. (2002) were done at an interval of 67 ms. The interval was too large so the details of flow may not be captured. Chao et al. (2009) investigated the maximum and average velocities but the velocity variation with time was not studied. The PIV studies by VanSciver et al. gave detailed flow information but with an even large interval of 267 ms. The efforts by Zhu et al. (2006) were also with a large interval of 70 ms. Therefore, none of these studies could be used to characterize the direction of a cough jet for CFD simulations. The measurements of the flow rate and direction must be performed with a frequency of 100 Hz or higher.

2.2 Mouth opening area during a cough

The area of mouth opening is required to obtain the velocity from the flow rate. The PIV studies by Zhu et al. (2006) indicated the peak cough velocity varied from 6 to 22 m/s with an average of 11.2 m/s. To our best knowledge little experimental studies were on

the area of mouth opening during a cough. Most researcher have assumed (Zhu et al., 2006, 2006; Zhao et al., 2005) the area to be a few square centimeters.

3. MEASUREMENT METHODS

The present study measured flow rates, flow directions and mouth opening areas of coughs. A spirometer based on Fleish type pneumotachograph (Sancho et al., 2004; Bongers et al., 2006) was used to measure the cough flow rates generated over time with a frequency of 330 Hz. The spirometer is consisted of numerous capillary tubes in parallel and gives the flow proportional to the pressure drop. It is based on Poiseuille's Law, which states that, under capillary conditions in a straight rigid tube, flow is proportional to pressure loss per unit length. The flow directions were visualized through moderate-speed photography (120Hz) with 1 Mega Pixel resolution. Cigarette smoke was used as seeding fluid. The cigarette smoke particle size is about 0.2 μm (Klepeis et al., 2002) in diameter and the measured temperature of the cigarette smoke was close to exhaled air temperature. Thus the exhaled smoke jet should closely follow the cough air jet profile. The mouth opening areas were measured through the moderate speed photography (120Hz). All the measurements were conducted with vertical head posture as shown in Fig.1. The head posture may affect the flow rate and flow direction in particular. But as the velocities during a cough are high, gravity effects may be negligible and the direction with respect to mouth may not change significantly.

All the measurements were performed over 12 female and 13 male subjects to obtain realistic flow features with an approval from the Institutional Review Board for human subject experimentation. Normal healthy subjects were recruited for the study. The subjects were first given an overview of the research and were told about the risk involved in the measurements. Every subject signed a consent form before proceeding for the measurements.

The flow rate measurements were done by placing a mask on subject's face. The mask had ports for mouth and nose and the ports were connected to a filter then further to the spirometer as shown in Fig 2.



Fig. 2 A subject with a mask holding the spirometer during test

Two types of flow measurements, single cough and sequential cough, were conducted. The single cough coughed just once while sequential cough coughed twice. Each test was repeated three times for every subject.

The flow visualization study was performed on smoker subjects. A light source was placed beneath a subject face to throw light upwards. The light source along with a dark background helped the flow visualization. The subjects were asked to exhale smoke out through coughing.

The measurements of mouth opening area were performed over 8 male and 8 female subjects. The subjects were asked to cough and the front views close to their lips were captured for the whole event.

4. RESULTS

This section presents the experimental results obtained from this investigation.

4.1. Flow rate of a cough

The flow rate characteristics of a cough are to develop a simple mathematical model describing the boundary conditions for CFD simulations.

Single cough

Fig. 1 shows the flow rate generated from a typical cough over time from a subject. The results indicate that the cough began with a very short inhalation (<1% of the total exhaled air volume), a very high acceleration afterwards in exhalation and subsequently a decay. The inhalation volume was very small and may be neglected.

Fig. 3 illustrates the transient flow of a cough for all the subjects studied. A large variation existed among the subjects. For example, the difference between the maximum and minimum values of CPFR, CEV and PVT for the male subjects was about 200%, 300% and 100%, respectively. The total inhaled volume during a cough was less than a percent of the total exhaled volume during a cough. The velocity during the inhalation period was also low. Table 1 summarizes the variation range of the CPFR, PVT and CEV for the subjects that were much diversified. Thus, the cough flow characteristics from a subject can not be used to represent the whole population that means a standard cough does not exist.

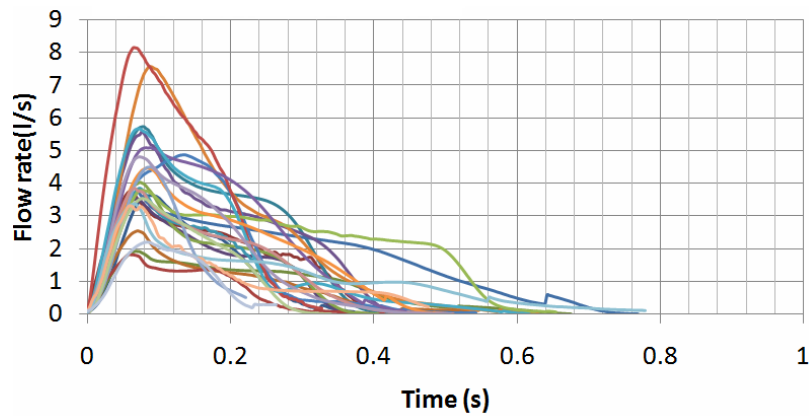


Fig. 3 Cough flow rates for the 25 subjects

Table 1 Variation observed in cough flow characteristics

	Male	Female
CPFR	3 - 8.5 l/s	1.6 -6 l/s
CEV	400-1600 ml	250-1250ml
PVT	57 - 96 ms	57 - 110 ms

To describe the flow characteristics, this study used non-dimensional parameters. The flow rate was non-dimensionalized by CPFR while the time by PVT as:

$$\overline{M} = \frac{Flowrate}{CPFR} \quad (1)$$

$$\tau = \frac{Time}{PVT} \quad (2)$$

Fig. 4 is exactly the same as Fig. 3 but in non-dimensional form. With the re-arrangement, one can see that when $\tau < 1.2$ all the curves are coincident. After that

time the variation existed but the trend looks similar. Moreover it can be seen that the dimensionless flow rate variation with time closely follows a gamma-probability-distribution function till about 1.2 dimensionless time. By superimposing another gamma-probability-distribution function the inflation zone including the cough flow rate decay can be captured. Equations (3) and (4) show these functions. Finally a non-linear least square curve fitting analysis was performed in MATLAB to obtain the optimum values of the variables required to define the gamma probability distribution function for each cough.. Eq. (3) for $\tau < 1.2$ that contains only CPFR and Eq. (4) for $\tau \geq 1.2$ that contains CPFR, PVT and CEV.

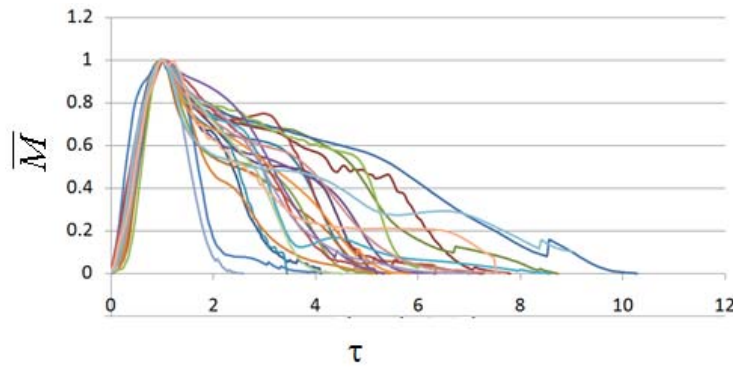


Fig. 4 Dimensionless cough flow rates from the 25 subjects

$$\bar{M} = \frac{a_1 \tau^{b_1-1} \exp(-\tau/c_1)}{\Gamma(b_1)c_1^{b_1}} \quad \text{for } \tau < 1.2 \quad (3)$$

$$\bar{M} = \frac{a_1 \tau^{b_1-1} \exp(-\tau/c_1)}{\Gamma(b_1)c_1^{b_1}} + \frac{a_2 (\tau-1.2)^{b_2-1} \exp(-(\tau-1.2)/c_2)}{\Gamma(b_2)c_2^{b_2}} \quad \text{for } \tau \geq 1.2 \quad (4)$$

where,

$$a_1 = 1.680$$

$$b_1 = 3.338$$

$$c_1 = 0.428$$

$$a_2 = \frac{CEV}{PVT \times CPFR} - a_1 \quad (5a-e)$$

$$b_2 = \frac{-2.158 \times CEV}{PVT \times CPFR} + 6.832$$

$$c_2 = \frac{1.8}{b_2 - 1}$$

Fig. 5 compares the measured flow rate with the fitted one obtained from equations (3) and (4) for a subject. Such a good agreement was found for all the subjects.

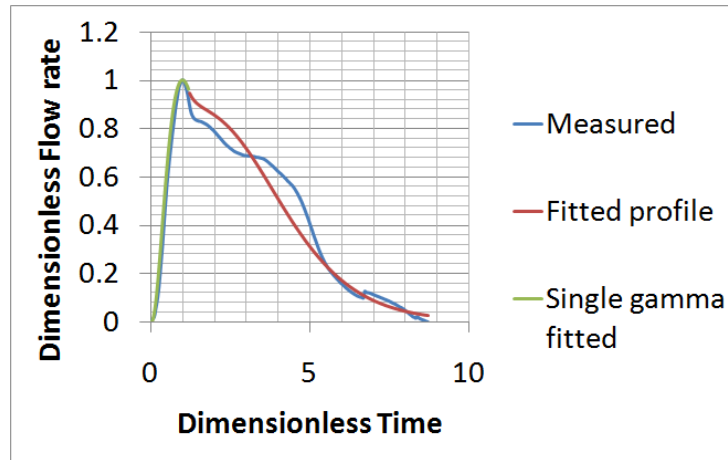
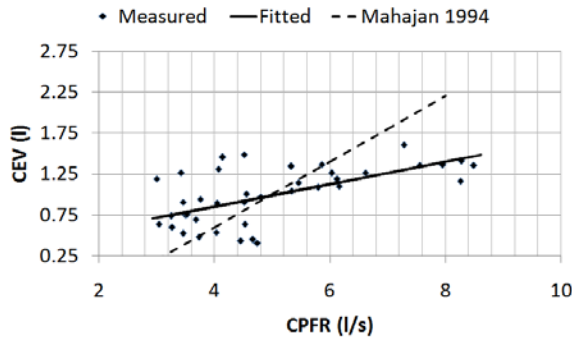


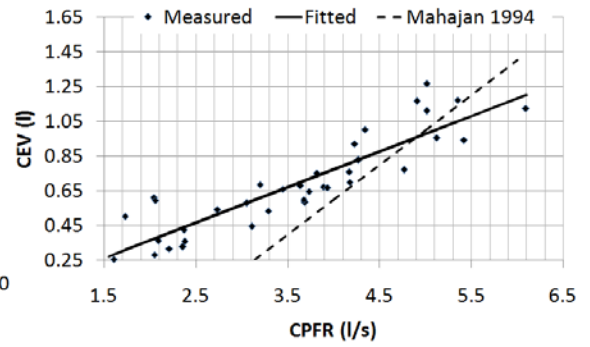
Fig. 5 Comparison of the flow rate calculated by Eqs. (3) and (4) for a single cough from a subject with the measured data

Please note that the CPFR, PVT and CEV are unknown for a new subject. In order to apply the two equations to a new subject, it is essential to link these variables to the subject's characters, such as height, weight, and gender. Our regression analysis by the solid lines shown in Fig. 6 indicates that these medical parameters were inter-related. Figs. 6(a) and 6(b) show the variation of the CEV with the CPFR for the male and female subjects, respectively. The figures show a positive correlation between all the parameter ($r > 0.5$, $p < 0.005$ for all). Since the CEV increases with the CPFR, this implies that the higher the peak flow rate the higher would be the total volume exhaled. The CPFR for the female subjects were lower than that for the male subjects. Mahajan et al. (1994) proposed using a single equation to correlate the CEV with the CPFR for both genders. As shown in Fig. 6, their regression lines deviate significantly from our data. Our two regression lines that distinguish the genders fit the best to the data.

Similarly, Figs. 7(a) and 7(b) show the variation of the PVT with the CPFR for the male and female subjects, respectively. The results again indicate that the PVT increased with the CPFR. The PVT for the female subjects was higher than that for the male subjects. This could be attributed to the difference in their larynx sizes as indicated by Singh et al. (1995). The slope of the PVT versus the CPFR variation is similar to that obtained by him, but the intercept is higher by about 50 ms in our measurements. Our measurements were performed at 330 Hz and can capture the initial period, which could have got missed out in previous studies.

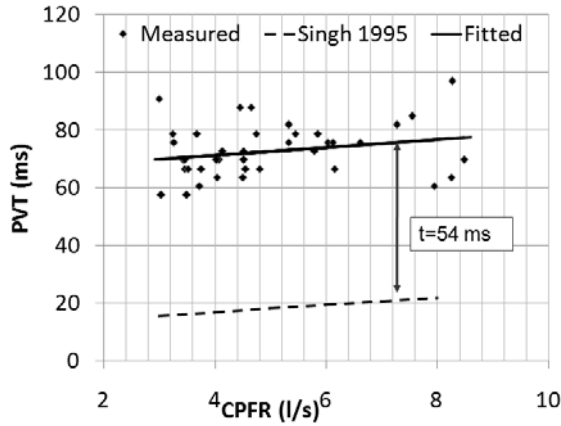


(a)

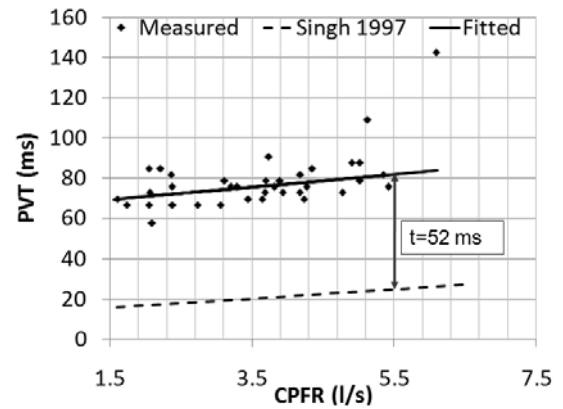


(b)

Fig. 6 The relationship between CEV and CPFR for (a) male subjects and (b) female subjects



(a)



(b)

Fig. 7 The relationship between PVT and CPFR for (a) male subjects and (b) female subjects

The regression lines shown in Figs. 6 and 7 can be mathematically expressed as:

$$CEV(l) = 0.138CPFR(l/s) + 0.2983 \quad \text{for male} \quad (6)$$

$$CEV(l) = 0.204CPFR(l/s) - 0.043 \quad \text{for female} \quad (7)$$

$$PVT(ms) = 1.360CPFR(l/s) + 65.860 \quad \text{for male} \quad (8)$$

$$PVT(ms) = 3.152CPFR(l/s) + 64.631 \quad \text{for female} \quad (9)$$

With the two sets of equations and the CPFR, one can determine the cough flow rate over time by Eqs. (3) and (4). The CPFR is the peak flow rate of air coming for lungs during a cough, it should be related to the lung volume and the exhalation capacity of the person. The lung volume depends upon the height (Hepper et al., 1960), while the exhalation capacity depends on the weight and height (Goldman et al., 1959; Gehan et al., 1970) of the person. Thus CPFR should be related to the weight and height of the person. By using our data and multiple regression analyses, this study found that the CPFR depends mainly on subject height. For the male subjects, the subject weight has some impact on the CPFR as well. The regression analyses lead to the following two equations for calculating the CPFR from the height and weight of a subject:

$$CPFR(l/s) = -8.8980 + 6.3952h(m) + .0346w(kg) \quad \text{for male} \quad (10)$$

$$CPFR(l/s) = -3.9702 + 4.6265h(m) \quad \text{for female} \quad (11)$$

The two equations can calculate the CPFR with an error no greater than 20% by comparing it with the data in our database. The equations indicates that the CPFR increases with the height and weight of the subject.

From the physiological information such as the height, weight, and gender, the CPFR can be calculated using equations (10) and (11). The CEV and PVT can be calculated from the CPFR using equations (6) to (9). With the CPFR, CEV and PVT, the dimensionless flow rate can be obtained from equations (3) and (4). Equations (1) and (2) can be utilized to convert the dimensionless flow rate into the dimensional one. Hence, the flow rate over time for a single cough can be obtained from the physiological information.

Sequential cough

A sequential cough is defined one cough followed immediately by the other. Fig. 8 shows the flow generated for a sequential cough from a subject. The flow behavior for the two coughs in the sequential cough was similar to that of a single cough and can also be described by equations (3) and (4). The first cough closely followed the features of a single cough while the second one was a scaled down of the first one. Tables 2 and 3 compare the sequential coughs with the single coughs from the male and female subjects, respectively. The PVT for the two coughs in the sequential coughs was approximately the same as that of the single coughs while the CPFR and CEV for the second cough were approximately 0.5-.0.6 times of the single coughs.

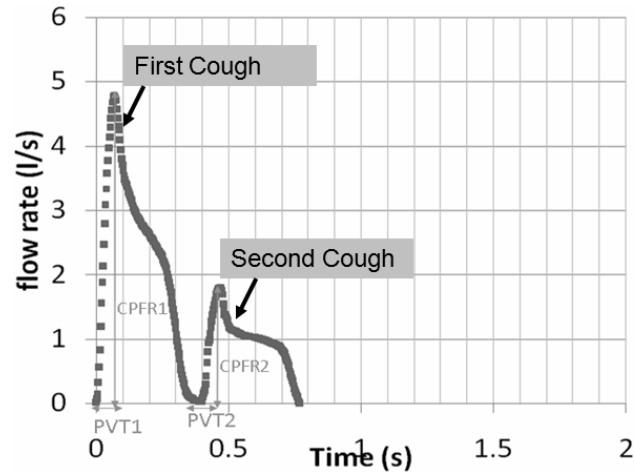


Fig. 8 Flow rate over time for a sequential cough from a subject

Table 2 Relationship between sequential and single coughs for the male subjects

	correlation with Single cough								
	CPFR			PVT			CEV		
	r	P	correlation	r	P	correlation	r	P	correlation
First cough	0.77	<.001	1.008*CPFR	0.58	<.001	1.105*PVT	0.6	<.001	0.8184*CEV
Second Cough	0.53	<.001	0.602*CPFR	0.33	<.001	0.9568*PVT	0.45	<.001	0.602*CEV

Table 3 Relationship between sequential and single coughs for the female subjects

	correlation with Single cough								
	CPFR			PVT			CEV		
	r	P	correlation	r	P	correlation	r	P	correlation
First cough	0.8	<.001	1.038*CPFR	0.7	<.001	1.107*PVT	0.63	<.001	0.8613*CEV
Second Cough	0.7	<.001	0.6335*CPFR	0.51	<.001	0.8697*PVT	0.55	<.001	0.5294*CEV

Thus, the CPFR, PVT and CEV for the first cough can be obtained from equations (6) to (11), while those for the second cough should be corrected with Tables 2 and 3. The flow rate can then be obtained by equations (3) and (4) for the two coughs.

4.2 Flow direction of a cough

The flow direction of a cough was obtained from flow visualization. Fig. 9 shows the sequence of images taken at 120 Hz for a typical cough process from $t=0$ to $36/120$ seconds. The first three images were for $t=0$ to $3/120$ seconds, when the mouth was closed. Then the images were from $t=9/120$ to $36/120$ seconds at an interval of $1/120$ seconds. At $t=9/120$ seconds, the mouth completely opened up but the smoke came out after $t=11/120$ seconds.

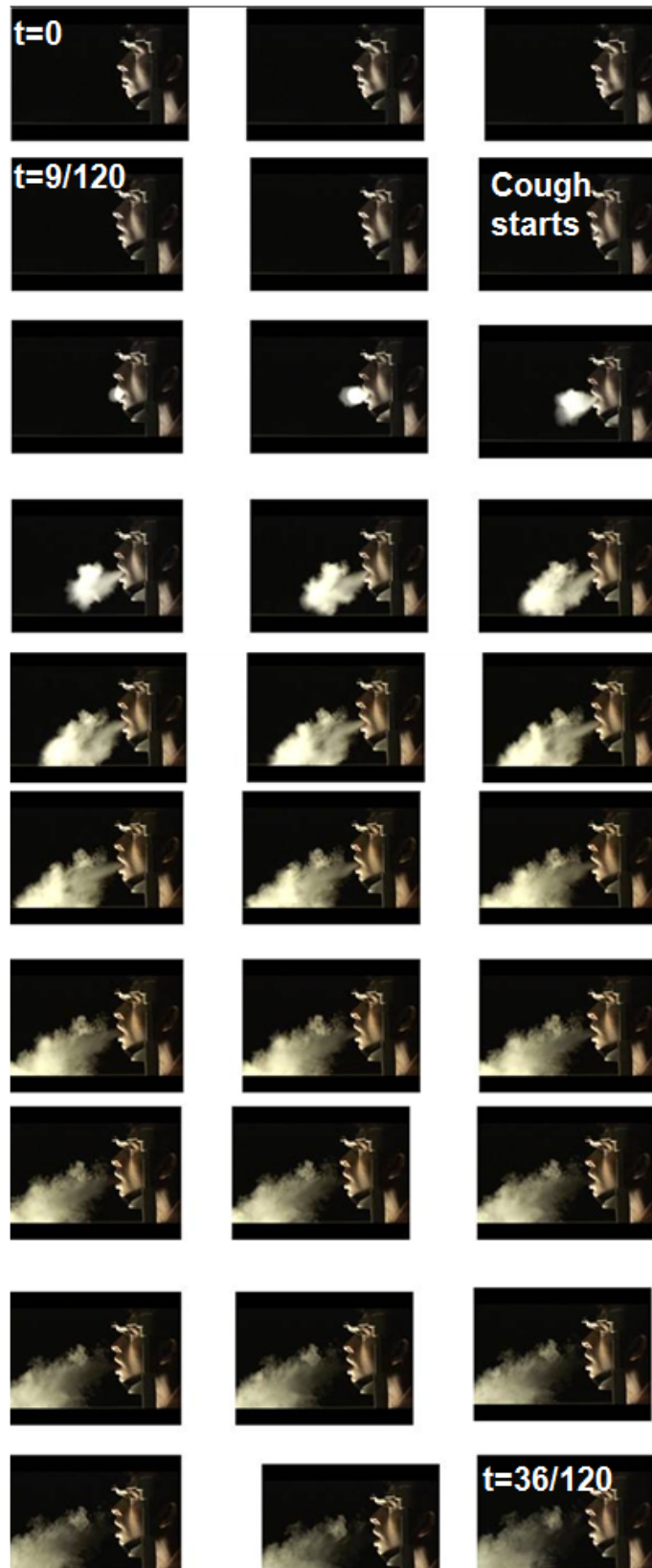


Fig. 9 The side view of a cough process recorded with a frequency of 120 Hz

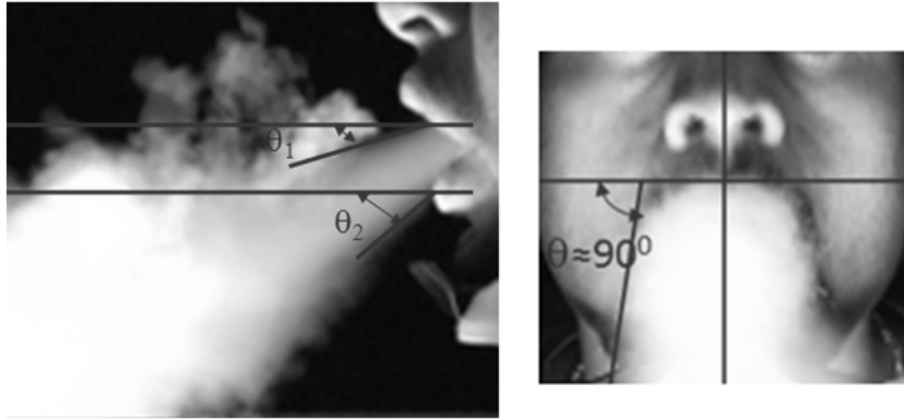


Fig. 10 The cough jet direction from the side and front views

The downward jet can be defined with two angles, θ_1 and θ_2 , as shown in Fig. 10. The jet has negligible spread in this view. Fig. 11 shows little variation in the cough angles for all the subjects. The 95% confidence bounds for the mean angles can be determined by

$$\theta_1 = 15^\circ \pm 5^\circ \quad (12)$$

$$\theta_2 = 40^\circ \pm 4^\circ \quad (13)$$

The two mean angles can be used as boundary conditions for CFD modeling.

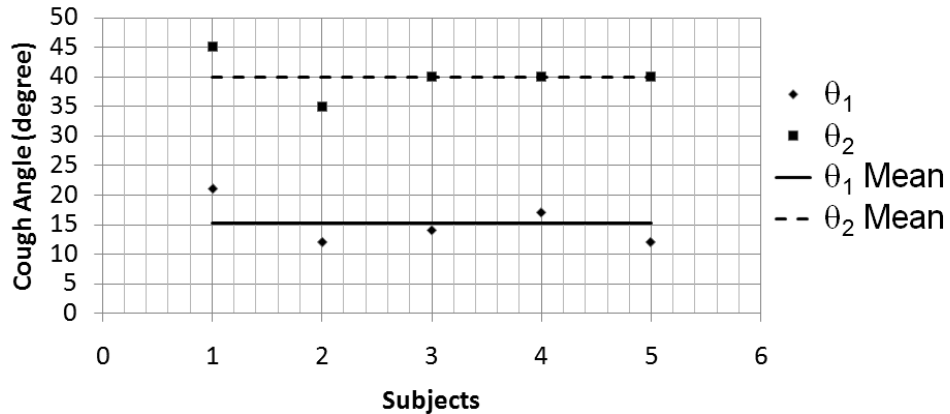


Fig. 11 Variation in the two cough angles among all the subjects

4.3. Mouth opening area

The mouth opening area is defined as the area between the lips during a cough. Fig. 9 shows the sequence of images during a cough. Initially the mouth was closed and then opened up fully at $t=9/120$ seconds. The mouth remained opened for the rest of the cough process. This can be further confirmed from the images of the front view for all

the subjects. Fig. 12 shows the mouth opening area over time for a subject. It can be seen that the mouth opening area was almost constant when there was flow from the mouth.

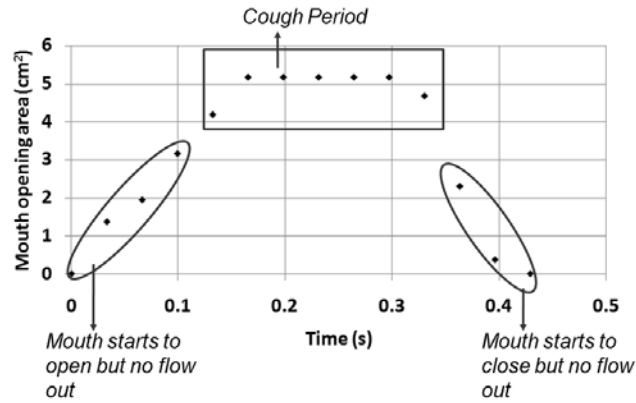


Fig. 12 Change of mouth opening area during a cough

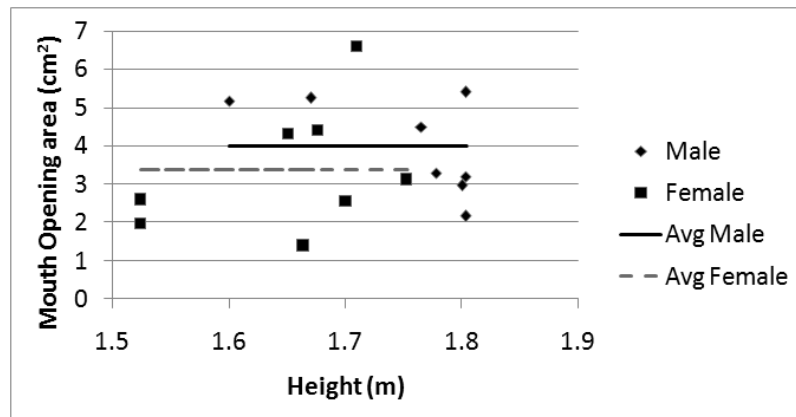


Fig. 13 Variation in mouth opening area during a cough with the heights of all the subjects

Fig. 13 shows the variation in mouth opening area during a cough with the heights of all the subjects. But the figure does not indicate any clear trend. Hence this study proposed to use an average value. The mean mouth opening area for the female subjects was smaller than that of the male subjects:

$$\text{Mouth opening area} = 4.00 \pm 0.95 \text{ cm}^2 \text{ for male} \quad (14)$$

$$= 3.370 \pm 1.40 \text{ cm}^2 \text{ for female} \quad (15)$$

4. DISCUSSION

This investigation has developed a set of simple equations that can be used to generate boundary conditions (or a source model) for predicting infectious virus transport by CFD due to coughing. Our effort focused on the flow rate, flow direction, and air velocity that can be determined from flow rate and mouth opening area. The inputs required are height, weight, and gender of a person.

The boundary conditions required by CFD simulations should also include the temperature of the exhaled air and the droplet distribution. The study by Hoppe (1981) can be utilized to obtain the exhaled air temperature under various ambient temperature and humidity. He found that ambient temperature is the most influential parameter. There are a few studies on cough droplet size measurements (Duguid, 1945; Fairchild et al., 1987; Papineni et al., 1997; Fenelly et al., 2004; Yang et al., 2007; Hersen et al., 2008; Chao et al., 2009; Morawska et al., 2009). The measurements were done over healthy subjects (Duguid, 1945; Fairchild et al., 1987; Papineni et al., 1997; Yang et al., 2007; Hersen et al., 2008; Chao et al., 2009; Morawska et al., 2009) and the subjects infected by TB (Fenelly et al., 2004) and with cough and cold (Hersen et al., 2008). The latest measurements (Yang et al., 2007; Hersen et al., 2008) indicated that the droplet concentration was of the order of 10^6 and the size varied from 0.1 to 10 μm . The study by Yang et al. (2007) indicated a linear trend with mean cough flow rate. Hence by knowing the mean cough flow rate from our model, the droplet concentration can be obtained.

5. CONCLUSIONS

This paper reports our effort to characterize the flow behavior of cough. The flow rate, flow direction and mouth opening area were measured for 25 human subjects, which could be used as boundary conditions in CFD simulations.

The flow rate can be defined as a combination of gamma probability distribution functions. The variables in the functions can be represented by medical parameter i.e. CPFR, PVT and CEV. These medical parameters are related to the height, weight, and gender of a person.

A sequential cough was found to be the combination of two single coughs. The first one behaved approximately the same as that of a single cough, while the second one was a scaled down version of the first one.

The cough flow direction was visualized through the moderate speed photography using smoke. The flow direction did not vary substantially among the subjects and can be determined by two angles.

The mouth opening area was constant during a cough. The mouth opening area varied among the subjects but without a clear correlation with the subject height. Hence this study proposed to use a mean mouth opening area during a cough.

6. REFERENCES

2002. *Bulletin of the World Health Organization*; 80 (3): 261.

Afshari, A., Azadi, S., Ebeling, T., Badeau, A., Goldsmith, WT., Weber, KC., Frazer, DG. (2002) Evaluation of cough using Digital Particle Image velocimetry. Proceedings of Second Joint EMBS-BMES Conference 23-26 October Houston TX IEEE, 975-976.

Badeau, A., Afshari, A., Goldsmith, WT., Frazer, D. (2002) Preliminary predictions of flow and particulate concentration produced from normal human cough dispersion. Proceedings of Second Joint EMBS-BMES Conference 23-26 October Houston TX IEEE, 246-247.

Bongers, T., O'Driscoll, BR. (2006) Effects of equipment and technique on peak flow measurements. *BMC Pulmonary Medicine*, 6-14.

Chao, CYH., Wan, MP., Morawska, L., Johnson, GR., Ristovski, ZD., Hargreaves, M., Mengersen, K., Corbett, S., Li, Y., Xie, X., and Katoshevski, D. (2009) Characterization of Expiration Air Jets and Droplet Size Distributions Immediately at the Mouth Opening. *J. Aerosol Sci*, 40, 122-133.

Cole, EC., Cook, CE. (1998) Characterization of Infectious Aerosols in Health Care Facilities: An Aid to Effective Engineering Controls and Preventive Strategies. *Am J. Infect. Control* , 26, 453-464.

Duguid, JP. (1945) The size and the duration of air-carriage of respiratory droplets and droplet-nuclei. *Journal of Hygiene*, 54, 471-479.

Edgerton, HE., Barstow, FE. (1959) Multiflash Photography. *Photographic Science and Engineering*, 3 (6), 288-291.

Edgerton, HE., Germeshausen, JK., Grier, HE. (1937) High speed Photographic methods of measurements. *Journal of applied Physics*, 2-9.

Fairchild, CI., Stamper, JK. (1987) Particle concentration in exhaled breath. *Am. Ind. Hyg. Assoc. J.*, 48, 948-949.

Fennelly, KP., Martyny, JW., Fulton, KE., Orme, IM., Cave, DM. et al. (2004) Cough generated aerosols of *Mycobacterium tuberculosis*: a new method to study infectiousness. *Am J Respir Crit Care Med*, 169, 604–609.

Gehan, EA., George, SL. (1970) Estimation of human body surface area from height and weight. *Cancer Chemother Rep.*, 54, 225-35.

Goldman, HI., Becklake, MR., (1959) Respiratory function tests; normal values at median altitudes and the prediction of normal results. *Amer. Rev. Tuberc. Pulm. Dis.*, 79(4), 457-467.

Hepper, NGG., Fowler, WS., Helmholz, Jr. HF. (1960) Relationship of height to lung volume in healthy men. *Chest*, 37(2), 314-320.

Hersen, G., Moularat, S., Robine, E., Gehin, E., Corbet, S., Vabret, A., Freymuth F. (2008) Impact of Health on Particle Size of Exhaled Respiratory Aerosols: Case-control Study. *Clean* 2008, 36(7), 572-577.

Holmes, NS., Morawska, L. (2006) A review of dispersion modelling and its application to the dispersion of particles: An overview of different dispersion models available. *Atmospheric Environment*, 40, 5902–5928.

Hoppe, P. (1981) Temperature of Expired Air under Varying Climatic Conditions. *International Journal of Biometeor*, 25, 127-132.

Jennison, MW. (1942) Atomizing of mouth and nose secretions into the air as revealed by high speed photography. *Aerobiology*, 17, 106-128.

Klepeis, NE., Nazaroff, WW. (2002) Characterizing size-specific ETS particle emissions, *Proceedings: Indoor Air*, 162-167

Lamb, JM., Murty, GE., Slater, RM., Aitkenhead, AR. (1993) Postoperative laryngeal function assessed by tussometry. *British Journal of Anesthesia*, 70, 478-479.

Leiner, GC., Abramowitz, S., Small, MJ., Stenby, VB. (1966) Cough peak flow rate. *The American Journal of the Medical Sciences* February, 251 (2), 211-214.

Mahajan, RP., Singh, P., Murty, GE., Aitkenhead, AR. (1994) Relationship between expired lung volume, peak flow rate and peak velocity time during a cough manoeuvre. *British Journal of Anaesthesia*, 72 (3), 298-301.

Morawska, L. (2006) Droplet fate in indoor environments, or can we prevent the spread of infection? *Indoor Air*, 16, 335-347.

Morawska, L., Johnson, GR., Ristovski, Z., Hargreaves, M., Mengersen, K., Chao, CYH., Li, Y., and Katoshevski, D. (2009) Size Distribution and Sites of Origins of Droplets Expelled from the Human Respiratory Tract During Expiratory Activities. *J. Aerosol Sci.*, 40, 256-269.

Papineni, RS., Rosenthal, FS. (1997) The size distribution of droplets in the exhaled breath of healthy human subjects. *J Aerosol Med.*, 10, 105-116.

Sancho, J., Servera, E., Diaz, J. (2004) Comparison of peak cough flows measured by pneumotachograph and a portable peak flow meter. *American Journal of Physical Medicine & Rehabilitation*, 83(8), 608-612.

Settles, GS., Hackett, EB., Miller, JD., Weinstein, LM. (1995) Full-Scale Schlieren Flow Visualization. *Flow Visualization VII*, ed. J. P. Crowder, Begell House, New York, Sept. 1995, 2-13.

Singh, P., Mahajan, RP., Murty, GE., Aithkenhead, AR. (1995) Relationship of peak flow rate and peak velocity time during voluntary coughing. *British Journal of Anaesthesia*, 74 (6), 714-716.

Sze To, GN., Wan, MP., Chao, CYH., Wei, F., Yu, SCT., and Kwan, JKC. (2008a) A Methodology for Estimating Airborne Virus Exposures in Indoor Environments Using the Spatial Distribution of Expiratory Aerosols and Virus Viability Characteristics. *Indoor Air*, 18, 425-438.

VanSciver M, Miller S, Hertzberg J. Particle Image Velocimetry of Human cough. Mechanical Engineering Department University of Colorado, Boulder CO.

World Bank 2005.

<http://web.worldbank.org/WBSITE/EXTERNAL/NEWS/0,,contentMDK:20715408~pagePK:64257043~piPK:437376~theSitePK:4607,00.html>

WHO 2004. "WHO guidelines for the global surveillance of severe acute respiratory syndrome (SARS)" Department of Communicable Disease Surveillance and Response, World Health Organization.

Yang, S., Lee, GWM., Chen CM., WU, CC., Yu, KP. (2007) The size and concentration of droplets generated by coughing in Human Subjects. *Journal of Aerosol Medicine*, 20(4), 484-494.

Zhao, B., Zhang, Z., Li, X. (2005) Numerical Study of Transport of droplets or particles generated by respiratory system indoors. *Building and Environment*, 40 (8), 1032-1039.

Zhu, S., Kato, S., Yang, JH. (2006) Investigation into airborne transport characteristics of air-flow due to coughing in a stagnant room environment. American Society of Heating, Refrigerating and Air-Conditioning Engineers Transaction, 112, 123-133.

Zhu, S., Kato, S., Yang, JH. (2006) Study on transport characteristics of saliva droplets produced by coughing in a calm indoor environment. Building and Environment, 41, 1691-1702.